IEEE Access
Multidisciplinary : Rapid Review : Open Access Journal

Received July 2, 2021, accepted August 19, 2021, date of publication August 24, 2021, date of current version August 30, 2021.

Digital Object Identifier 10.1109/ACCESS.2021.3106880

A Localization and Navigation Method for an In-Pipe Robot in Water Distribution System Through Wireless Control Towards Long-Distance Inspection

SABER KAZEMINASAB[1], (Graduate Student Member, IEEE), AND M. KATHRINE BANKS[2]
[1]Department of Electrical and Computer Engineering, Texas A&M University, College Station, TX 77847, USA
[2]College of Engineering, Texas A&M University, College Station, TX 77847, USA

Corresponding author: Saber Kazeminasab (skazeminasab@tamu.edu)

ABSTRACT In this paper, we propose an operation procedure for our previously developed in-pipe robotic system that is used for water quality monitoring in water distribution systems (WDS). The proposed operation procedure synchronizes a developed wireless communication system that is suitable for harsh environments of soil, water, and rock with a multi-phase control algorithm. The new ''wireless control algorithm'' facilitates ''smart navigation'' and ''near real-time wireless data transmission'' during operation for our in-pipe robot in WDS. The smart navigation enables the robot to pass through different configurations of the pipeline with long inspection capability with a battery in which is mounted on the robot. To this end, we have divided the operation procedure into five steps that assign a specific motion control phase and wireless communication task to the robot. We describe each step and the algorithm associated with that step in this paper. The proposed robotic system defines the configuration type in each pipeline with the pre-programmed pipeline map that is given to the robot before the operation and the wireless communication system. The wireless communication system includes some relay nodes that perform bi-directional communication in the operation procedure. The developed wireless robotic system along with operation procedure facilitates localization and navigation for the robot toward long-distance inspection in WDS.

INDEX TERMS In-pipe robots, wireless control algorithm, smart navigation, water quality monitoring, water distribution systems.

I. INTRODUCTION

Water Distribution Systems (WDS) are responsible to carry potable water to residential areas. Aging pipelines cause leaks and water loss in the system. The amount of water loss is unavoidable; around 15%-25% and 20% of the purified water is reported for water loss in the US and Canada, respectively [1], [2], Hence, it is required to periodically assess the condition of pipelines and localize the leak location. The traditional methods for leak detection primarily depend on user experience [3]. In addition to condition assessment and leak detection, utility managers need to measure water parameters periodically to ensure the health of the water. However, it is an extremely challenging task to access all parts of the distribution network as the pipelines are long, composed of complicated configurations, and commonly buried beneath the earth's surface. Mobile sensors that are designed to go inside pipes are not feasible to use as their motion depends on flow in the pipe and the user loses them in the network during operation [4], [5]. In-pipe robots are designed to solve the problem of passiveness of mobile sensors, in which actuator units and control algorithms control their motion to be independent of water flow. They move inside pipes and perform desired tasks (e.g. leak detection or quality monitoring) [6] and are powered by either cable [7] or battery [8]. Due to the long length of pipelines and the short length of cables, the feasibility of tethered robots are limited. As a result, battery-powered robots are desirable for long pipeline inspection. The battery-powered in-pipe robots communicate with the base station above ground through wireless communication [9]. However, due to high path loss and dynamic communication links of soil, rock, and water, wireless communication is a

The associate editor coordinating the review of this manuscript and approving it for publication was Christopher H. T. Lee.

challenging task in these environments [10] and [11]. This makes the range of coverage of current communication setups limited and it is not possible to cover all parts of the network with one pair of transceivers. To address the problem of limited coverage, the idea of relay nodes is introduced in the literature [12] in which some transceivers are placed above ground and relay the data between robotic sensors and base station above ground. Relay nodes are usually used for fixed sensor networks [13]. A team from the Massachusetts Institute of Technology (MIT) has used the idea of relay nodes in in-pipe robotic sensors and coined the term ''wireless robotic sensors'' for the localization of the robot [14]. Wireless robotic sensors are advantageous over other methods as longer distances of the network can be inspected while the sensor measurements can be transmitted during operation. There are also other localization and navigation methods for in-pipe robots that remove the need for wireless communication in which work based on the information from the surrounding environment using ultrasonic sensors [15], camera [16], or laser rangefinder [17] sensors. The information from these sensors is used with the recent numerical methods (e.g. Kalman filter and Particle filter) to estimate the location of the in-pipe robot. In [18], the authors use a hydrophone and the RaoBlackwellised particle filter (RBPF) to localize the robot in the pipeline and also create the map of the pipeline at the same time (simultaneous localization and mapping (SLAM)). The non-straight configurations of the pipelines (e.g. bends or Tees) can be used for localization as landmarks. Using a vision-based landmark detection technique, the authors in [19] developed a pattern-matching image-processor method to recognize the shadow of elbows and branches in pipelines. However, the drawbacks of the systems without wireless systems are twofold: it is not possible to transceive data between the robot underground and the base station above ground during operation, and also, since there is no connection to the robot during operation, if a failure of motion occurs during operation, it is not possible to localize the stuck robot in pipeline. Hence, these methods limit the traveling distance of the in-pipe robots.

A. TECHNICAL GAP

Pipelines are composed of different configurations like bends and T-junctions in which the robot needs to pass through them to facilitate long pipe inspection. To the best of our knowledge, there is not a method to localization and navigation in chattered and complicated environment of in-service pipelines with long distance inspection. Also, it is desired the in-pipe robot perform regular measurement of water parameters (e.g. turbidity, conductivity) or pipe parameters (e.g. pressure gradient) during operation that is not well-addressed in the literature.

B. OUR CONTRIBUTION

In this research:

1) We improve our previously designed in-pipe robot [9] for locating the electronic parts indie the central processor.

2) We propose a bidirectional low-frequency wireless system and synchronize it with the micro-pump system and motion control unit.

3) We propose a localization method to localize the robot in complicated configurations of pipelines.

4) We propose a navigation method to enable the robot to move in complicated configurations of the pipeline.

5) We develop an operation procedure for the robotic system that facilitates regular measurements of health-related parameters in water for long-distance inspection.

The remainder of the paper is organized as follows: In Section II, the design of the modular in-pipe robot is present, modeled, and characterized. In Section III, the wireless sensor module is developed and validated. In section IV, the operation procedure for the robotic wireless is presented and verified with the experimental results. The paper is concluded in Section V.

II. ROBOT DESIGN AND CHARACTERIZATION

A. DESIGN

Our proposed robot is composed of:

- A Central Processor.
- Three Arm Modules.
- Three Actuator Modules.

Three arm modules are connected to the central processor at 120° angles and make the outer diameter of the robot adaptable to the pipe diameter (9 in-22 in).

The robot moves inside the pipe by actuator modules that are connected at the end of the arm modules. Each actuator module comprises a gear motor, a motor cover, moldable glue, and a wheel. More detail on the design, characterization, and fabrication can be found in our previous work [20]. The central part is designed to locate the sensing, control, drive, wireless, and power units of the robot. The robot is self-powered and the battery is located below the control part and its power is transferred to other electronic units via wire. The electronic units (i.e. sensing, control, wireless, and drive units) are designed and printed on a printed circuit

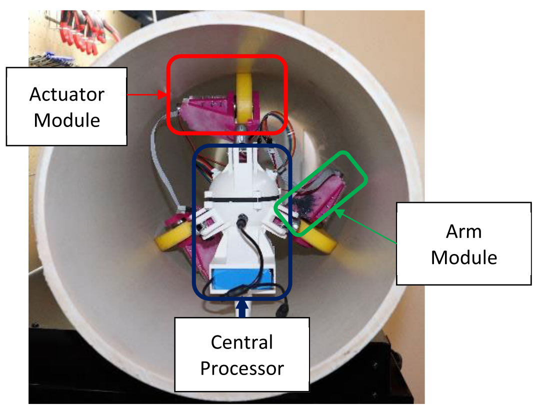

FIGURE 1. Our proposed self-powered in-pipe robot: [a] CAD design. [b] Robot in pipe. [c] Prototype of the robot in a pipe and the components: Actuator module, Arm module, and central processor.

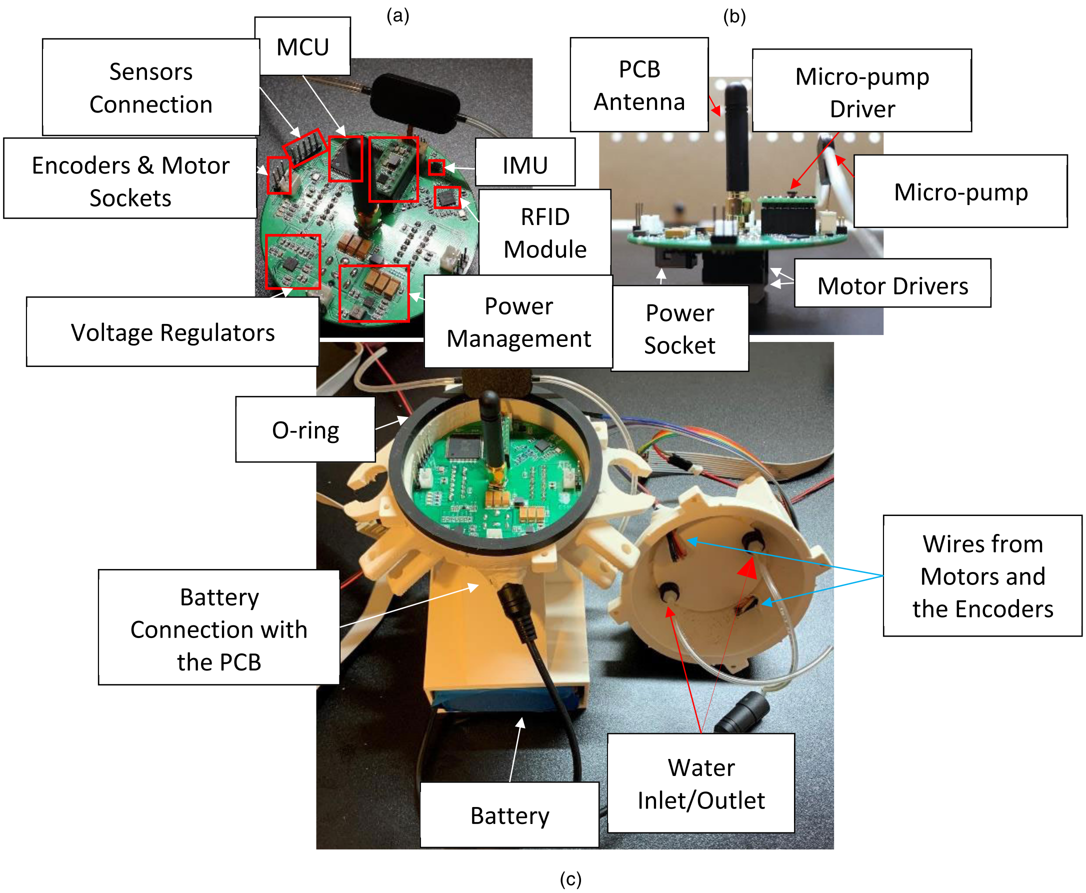

FIGURE 2. PCB and central processor. (a) Perspective view of the PCB. The sensors, encoders and the motors wires are connected to the PCB via headers. Three voltage levels of 12V, 5V, and 3.3V is available in the PCB via voltage regulators. (b) Side View of the PCB. Micro-pump system provides water sample to the water sensors for parameter measurements (e.g. PH, free-chlorine) and the timing for micro-pump is controlled via the MCU and the micro-pump driver. (c) PCB Location in the Central Processor and its Connection with the Battery. The wireless from the motors and the Water inlets and outlets are defined in the figure.

board (PCB). A micro-pump system provides water samples for the sensors in the central processor through water inlets and outlets and its function (i.e. timing) is controlled with the micro-pump driver. Fig. 2 shows the improved central processor, the PCB and its location the central processor. We took health considerations into account during the design of the robot in which the components inside the central processor and the actuator modules are isolated from the outside environment and also the components of the robot do not react chemically with water. In addition, they do not release toxic material into water. So, the robot is waterproof and can be inserted in the pipelines in which potable water is present. The dynamic of the robot can be presented with the following equations [21].

B. CHARACTERIZATION

There is a notion of resilient machine that accounts for the requirements to design a system that is robust against the undesired disturbances and uncertainties [22]. In this regard, we defined the condition where the robot fails during operation and improve the design to prevent failure. The robot is supposed to operate in in-service networks that are pressurized and water flow is present. Hence it is important that the motion of the robot is independent of flow motion. In our robot, two components paly important role in the design of automotive system: spring mechanism and battery capacity. In following, we characterize each component.

1) SPRING MECHANISM

Since the robot motion is based on wheel wall-press, friction force between the pipe wall and the wheels needs to be sufficient to have pure rolling and prevent slippage. We need to provide an analysis for the friction to prevent slippage of the wheel to have controlled motion. The friction is provided by the passive spring attached to each wheel (F_N and F'_N in Fig. 3a). Since the weight of the robot increases the normal force of the wheels that are below the center of mass of the robot (Fig. 3a), the required stiffness for the springs that are attached to these arms and wheels can be less than the required stiffness for the wheel that is above the center of

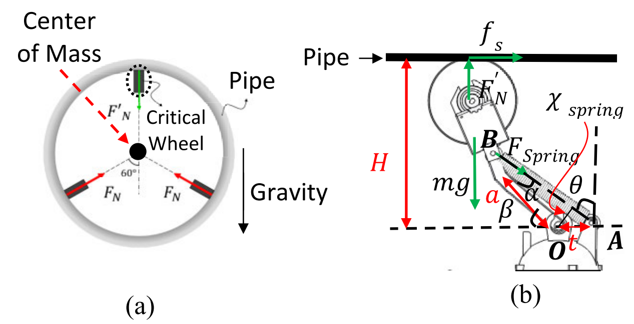

FIGURE 3. (a) The critical wheel. (b) Free body diagram of the critical wheel for static force analysis.

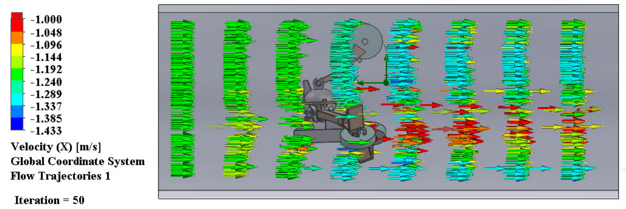

FIGURE 4. Flow simulation environment in solidworks.

mass (Fig. 3a). Hence, we provide the analysis for this wheel that is more likely to lose its contact with the pipe wall during motion. Based on Fig. 3b, we can write:

$$\sum M_O = 0 \rightarrow \left(mg - F_N'\right) a \cos\beta = f_s.H + F_{Spring}\chi_{Spring} \tag{1}$$

In triangle ***OAB***:

$$\beta = \alpha + \left(\frac{\pi}{2} - \theta\right) \tag{2}$$

$$\alpha = \sin^{-1}\left(\frac{t}{a}\cos\theta\right) \tag{3}$$

From (2) and (3), we have:

$$\beta = -\theta + \sin^{-1}\left(\frac{t}{a}\cos\theta\right) + \frac{\pi}{2} \tag{4}$$

Also, we can write:

$$\beta = \sin^{-1}\left(\frac{H}{L}\right) \tag{5}$$

Plugging (5) to (4):

$$\sin^{-1}\left(\frac{H}{L}\right) = -\theta + \sin^{-1}\left(\frac{t}{a}\cos\theta\right) + \frac{\pi}{2} \tag{6}$$

In (6), θ is calculated with a nonlinear trigonometric relation based on pipe radius, H. We also have:

$$\chi_{Spring} = t\cos\theta \tag{7}$$

Plugging (7) and (6) into (1):

$$F_{Spring} = \frac{1}{t\cos\theta}\left(\left(F_N' - mg\right) a\cos\right. \times \left.\left(\theta + \sin^{-1}\left(\frac{t}{a}\cos\theta\right)\right) - f_s H\right) \tag{8}$$

The springs are linear where the relation between force, F_{Spring}, and displacement for them are linear. The displacement is calculated between the points where $\theta = 0$, $\sqrt{(t+\cos\beta)^2 + (a\sin\beta)^2}\cos\theta$ and $\theta > 0$, $\sqrt{(t+\cos\beta)^2 + (a\sin\beta)^2}$ (triangle ***OAB***). Hence:

$$F_{Spring} = K\left(\sqrt{(t+\cos\beta)^2 + (a\sin\beta)^2}\right)(1-\cos\theta) = KU(\theta) \tag{9}$$

From (8) and (9):

$$K = \frac{1}{t}\cos\theta\,(U(\theta)) \times \left(\left(F_N' - mg\right) a\cos\left(\theta + \sin^{-1}\left(\frac{t}{a}\cos\theta\right)\right) - f_s H\right) = G(\theta) \tag{10}$$

To acquire pure rolling, we have:

$$K = max\,(G(\theta)) \tag{11}$$

In addition, (12) that is coulomb friction force relation needs to be satisfied:

$$f_{s(\max)} = \mu_s F_N' \tag{12}$$

where μ_s is friction coefficient and is 0.8 for pipe wall and wheel contact [9]. We need to find a value for $f_{s(\max)}$. It needs to be greater than the maximum traction force that each wheel needs to provide and to calculate the maximum traction force, we performed flow simulation with computational fluid dynamics (CFD) work in SolidWorks to compute the maximum resistive force against the robot. In this scenario, the robot moves with 50 cm/s velocity in the opposite direction of flow motion with 70 cm/s velocity; the outer diameter of the robot is 22-in that is its maximum diameter for it and the line pressure is 100 kPa (standard line pressure). Table 1 shows the simulation specifications and Fig. 4 shows the simulation environment. The colored lines show the velocity counter around the robot in the pipe. In this scenario, the drag force is computed around 26.1 N that the wheels should provide. Since the geometry of the robot is symmetric, each wheel needs to provide one-third of the maximum drag force (i.e. 8.7 N). Hence the value for traction force is 8.7 N that is equal to $f_{s(\max)}$ and based on (12), $F_N' = 11$ N. We calculated the required stiffness in each pipe

TABLE 1. Flow simulation specifications.

Parameter [unit]	Value
Fluid Type	Water
Robot Velocity [cm/s]	50
Flow Velocity [cm/s]	70
Pipe Diameter [in]	22
Relative Direction of Robot and Flow Motion	Opposite
Line Pressure [kPa]	100

diameter based on (14) and the results are shown in Fig. 5. To cover all pipe diameters, we selected the maximum value for K which is the required stiffness in 22-in diameter with the value of 3.35 kN/m. Hence, we calculated the value for the spring stiffness based on the maximum drag force that is computed in the CFD work and provides sufficient normal force for the wheels for pure rolling. The spring stiffness for all springs is equal.

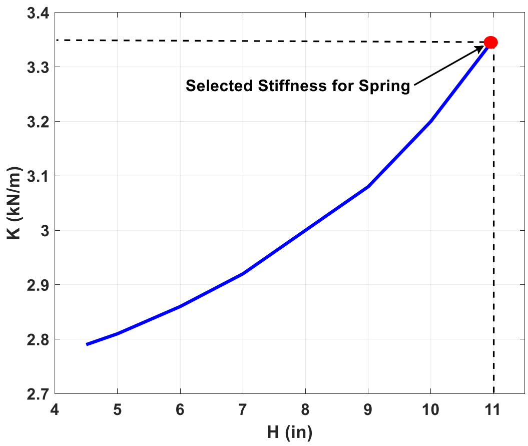

FIGURE 5. Stiffness value calculation for pure rolling of wheels during operation in different sizes of pipe in size-adaptability range of the robot and selected value for stiffness.

2) BATTERY

The other important factor for autonomous robot is battery capacity. We calculated the battery capacity with (13):

$$C = \frac{3P.h}{V_n} \tag{13}$$

where C (A.h), $P = 20$W, h (hour), and $V_n = 12$ V are battery capacity, gear-motor power, assumed operation duration, and gear-motor operating voltage. In this method, an operation procedure is assumed and battery capacity is calculated and a battery is selected. Then, the drawn current from the battery by gear-motors (at the operating point for traction force of 8.7N in the CFD work) is defined. The discharge time of the battery at this drawn current and voltage (12 V) is defined and compared with the assumed operation duration. If they are approximately equal, the battery capacity and the operation duration are realistic, otherwise, we need to consider another operation duration and repeat the process. In our system, the battery capacity is calculated around 15 A.h and the operation duration is around 3 hours.

3) DISCUSSION

The improved robot locates the designed PCB in the small space of the central processor and isolates it electronically. Also, the actuator module is waterproof that prevents damage to the gear motors. The spring mechanism and the battery of the robot are characterized to prevent failure during operation considering the maximum drag force applied on the robot that is computed with CFD work.

TABLE 2. Wireless sensor module specifications.

Parameter [unit]	Value or Description
Physical Layer	CC1200
Carrier Signal Frequency [MHz]	434
Antenna	Taoglas TI.10.0111 (SMA Mount)
MCU	ATMEGA2560
Number of Sensors	Up to 5
Unit 1	Micro-pump System
Unit 2	Motion Control

III. WIRELESS SENSOR MODULE

Our in-pipe robot is self-powered and needs communication with the base station to exchange sensors' data and motion control commands through wireless communication. In this application, the robot moves inside the pipeline and the transceiver(s) are located outside the pipe (above ground) a few meters away from the robot (we will later explain the location of transceivers in this paper). The robot switches its communication between transceivers during operation. Hence, there is a need for fast discovery between the robot and the transceivers. Also, we need a bi-directional wireless system that facilitates data transmission on both sides (i.e. from the robot to the base station and from the base station to the robot). However, wireless communication in underground applications is challenging since the environments of water, pipe, and soil attenuate radio signals (i.e. high path loss) [10], and also the communication channel is dynamic in which the volumetric water content and also the sand-clay composition in soil are variable and affect the path loss in soil [10]. To mitigate high path loss, low-frequency carrier signals for wireless communication are desired [10].

Considering the aforementioned requirements, we propose a wireless sensor module based on radio frequency identification (RFID) technology that can operate in low carrier frequencies [23]. To this aim, we use CC1200 from Texas Instruments (TI) Inc©as the physical layer of the RFID module that facilitates bi-directional communication and works in five sub-1GHz frequency bands (i.e. 169, 434, 868, 915, and 920 MHz) [24]. Also, it has 128-byte data FIFO on the transmitter (TX) and 128-byte data FIFO on receiver (RX) sides that facilitate high data throughput in our application [25]. The functions of the CC1200 (e.g. data packet creation, the transmission of data, reception of data, etc.) are controlled with the host MCU [26]. Our wireless sensor module comprises the RFID module that is connected to the five sensors for up to five parameters measurement in water that is an improvement compared to our team's previous work [5] (one parameter measurement) and also comparable with [27] that perform five parameters measurement. The physical layer (i.e. CC1200) triggers one interrupt on the MCU's pin (GPIO in Fig. 6) upon reception and transmission of a data packet. We use this feature of the physical layer to control the function(s) of two units: the micropump system and the motion control unit. The micro-pump system provides

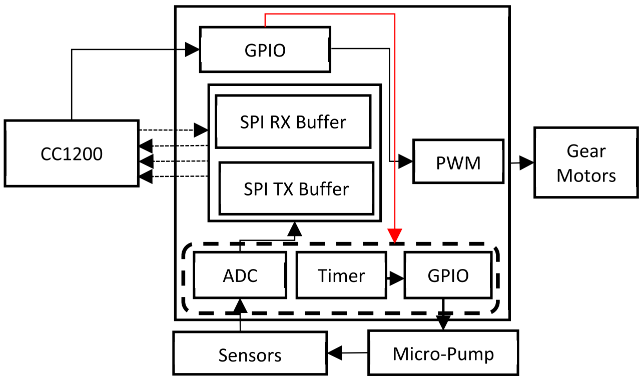

FIGURE 6. **Block diagram for the wireless sensor module.**

water samples for the sensors that need water samples for measurement (mp6, Bartels Mikrotechnik). When an interrupt occurs, the micro-pump starts circulating water in the sensors and the ADC of the MCU starts taking samples (dashed rectangular in Fig. 6). Also, the interrupt is connected to the motion of the control unit (Pulse Width Modulation (PWM) signals for the gear-motors). We will explain the details about the micro-pump and the motion control units, later in this paper. The wireless system in this system works in 434 MHz carrier frequency, the MCU is ATMEGA 2560, the antenna type is Taoglas TI.10.0111 with SMA mount, that are printed with other parts of the electronic components a circular printed circuit board (PCB) with 2.94-in diameter and located in the central processor (see Fig. 2c). Table 2 shows the specifications of the wireless sensor module.

A. FUNCTIONALITY OF THE WIRELESS SENSOR MODULE: BI-DIRECTIONALITY. FAST DISCOVERY CAPABILITY, AND MAXIMUM THROUGHPUT OF THE WIRELESS SENSOR MODULE

We mentioned earlier that we need bi-directional wireless communication, fast discovery capability between the robot and the transceivers, and high data throughput. In this section, we evaluate the performance of the proposed wireless sensor module in terms of bi-directionality, connection pick capability, and also measure the maximum data throughput. To this aim, an experimental setup is designed that is shown in Fig. 7. In this setup, five FlexiForce sensors ([c] in Fig. 7) are connected to the PCB of the robot ([f] in Fig. 7) and powered with the power supply ([d] in Fig. 7). The PCB is powered by a battery. Two transceiver modules ([a] and [b] in Fig. 7) are designed that each one includes an MCU Launchpad and CC1200 evaluation module. In each experiment in the following, a specific architecture of the setup in Fig. 7 is implemented to validate the desired functionality.

1) BI-DIRECTIONALITY

To evaluate the bi-directionality capability of the wireless sensor module to the transceiver, we performed two experiments: In the first experiment, the data packets are created in the wireless sensor modules and transmitted to the transceiver module 1. We sent 100 data packets and since an interrupt occurs on a designated pin upon reception of a data packet in transceiver module 1, it is supposed to see 100 interrupts on the pin in this experiment. We did and verified 100 interrupts on the 100 data packets on the transceiver module 1 with the logic analyzer.

In another experiment, the data packets are sent from the transceiver module 1 to the PCB and the same procedure is repeated and the same number of interrupts on the wireless sensor module's MCU and the transmitted data packets are verified. Hence, the interrupt capability of the wireless sensors module facilitates knowledge about the transmission and reception of data packets and also the number of data packets. Hence, we have a bi-directional wireless communication system in our application.

2) CONNECTION PICK CAPABILITY

The robot moves in the pipe and the transceivers are located outside the pipe. We have multiple transceivers in our application (we will elaborate more about this in this paper) and it is important for the wireless sensor module on the robot to easily establish communication with the transceivers when it reaches the read range of the transceivers. To evaluate the capability of fast discovery between the wireless sensor module and the transceivers, the wireless sensor module sends data packets to Transceiver Module 1, so we have communication between them and a graphical user interface (GUI) monitors the received packets (see Fig. 8a). During this transmission, transceiver module 2 at receive mode is added to the network and it is expected that the second transceiver also receives the same data packets as well. We realized that transceiver 2 receives the same data packets as transceiver 1 (see Fig. 8b). Hence, there is fast discovery between the transceivers and the wireless sensor module in this application.

3) MAXIMUM THROUGHPUT

The maximum data rate in our wireless system was measured to be around 120 kbps that is greater than similar wireless underground communication systems [28]–[30] and also sufficient for wireless underground applications [10].

4) SIGNAL PENETRATION IN WATER ENVIRONMENT

To evaluate the performance of the developed sensor module, we designed a prototype of the wireless system with CC1200 evaluation module in 434 MHz, Arduino MEGA 2560 REV3 (MCU), and five force sensors that are connected to the ADC channels of the MCU. The dynamic range of the force sensors are the same as the water sensors. The prototype is powered with battery, is located in a water resistant bag, and submerged in water (see Fig. 9). The wireless sensor module creates the data packets from the sensor measurements and sends them wirelessly with 14 dBm that is the maximum transmit power that the physical layer can transmit data [24] and the customized antenna (Taoglas TI.10.0111). In the first

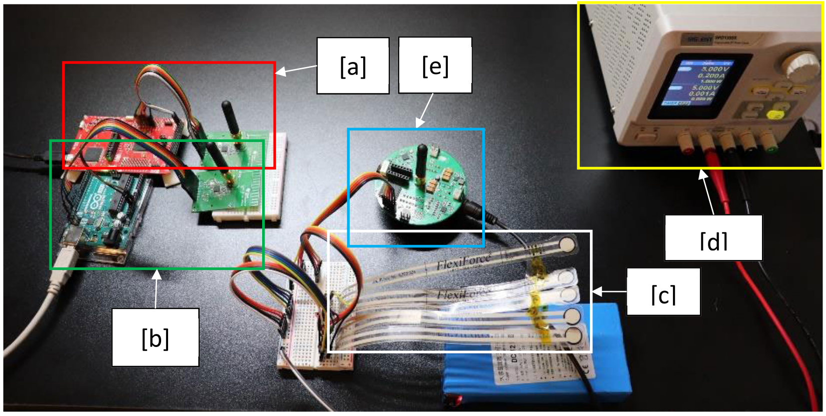

FIGURE 7. **Experiment station for the wireless sensor module functionality. [a] Transceiver module 1. [b] Transceiver module 2. [c] Five force sensors. [d] Power supply to power sensors. [e] PCB.**

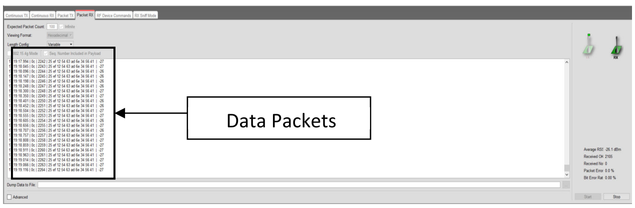

(a)

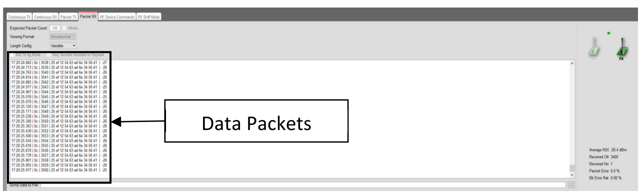

(b)

FIGURE 8. **Graphical user interface (GUI) for monitoring the received data packets for [a] Transceiver module 1, [b] Transceiver module 2.**

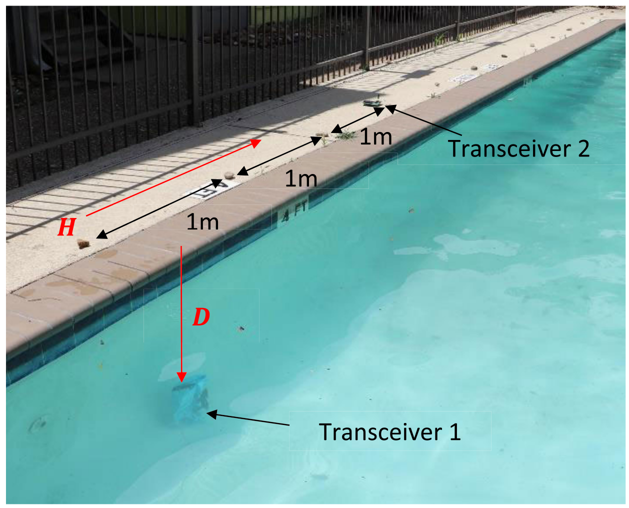

FIGURE 9. **The strength of the radio signal at water medium. Transceiver 1 is located in a water resistant bag and submerged in a bucket of water. The depth of water is 1 m and the transceiver 2 is located on the ground a moves horizontally. *D* is the vertical distance of transceivers and *H* is the horizontal distance between receivers.**

experiment, horizontal distance between the transceiver 1 and transceiver 2 is zero ($H = 0$) and vertical distance is increased ($D\uparrow$). The results in Fig. 10 shows that the RSS is decreased from -66 dBm at 10 cm to -82 dBm at 60 cm and comparing to the -100 dBm that is the threshold power for correct realization of radio signals based on [10]. In another experiment, the transceiver 1 is submerged in different values of depths and horizontal distances of the transceiver (see Fig. 11). The results show that RSS does not change when horizontal distance between the transceivers increased, however, it changes dramatically when the depth of transceiver 1 changes. Hence the distance of the transceivers in the air does not affect the RSS, however, the distance in the water medium affects the RSS substantially and we can conclude that the read range of the developed wireless module with the customized antenna is around 40 cm (15.75 in) that is aligned with the size adaptability of the robot for the pipe radius (4.5 in-11 in); in real application, the robot moves in pipe with water. The antenna of the wireless sensor module is located in the central processor that is located in the center of pipe full of water (see Fig. 12).

In this section, we developed a bi-directional wireless sensor module that works based on RFID module and customized antenna. It facilitates multi-parameter (five parameters) measurements and transmissions with maximum data rate of 120 kbps. The read range of the wireless sensor module is around 40 cm in water medium that is aligned with the size-adaptability of the robot.

IV. OPERATION PROCEDURE

So far, we have a size-adaptable in-pipe that is equipped with a bi-directional wireless communication system for pipe inspection in harsh environments in which signal attenuation is high. In this section, we propose an operation algorithm that synchronizes the wireless communication system with

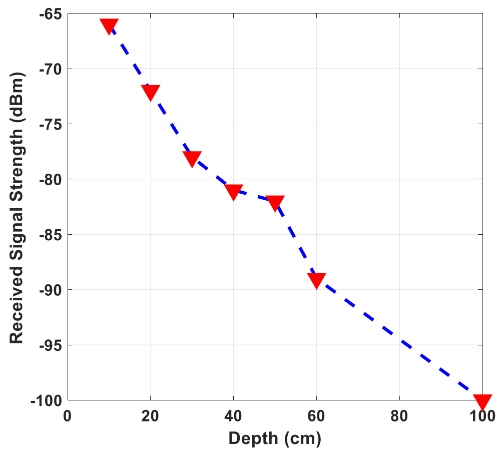

FIGURE 10. Received signal strength (RSS) at different vertical distances of transceiver 1 and transceiver 2.

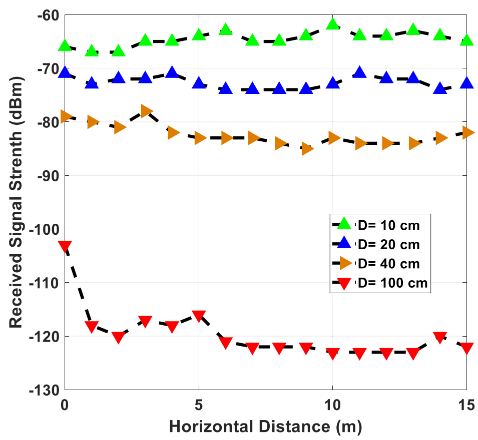

FIGURE 11. Received signal strength (RSS) at different horizontal and vertical distances of transceiver 1 and transceiver 2.

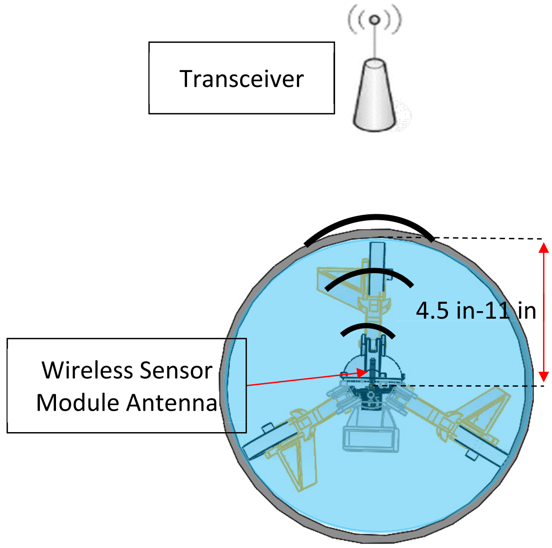

FIGURE 12. The location of the antenna in the central processor and the distance from the transceiver.

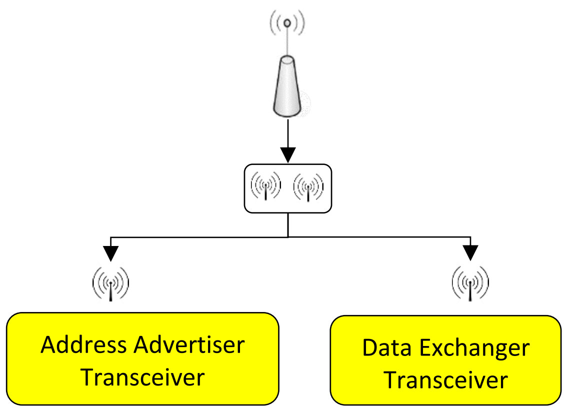

FIGURE 13. [a] Each relay node (RN) comprises two parts: Address advertiser transceiver (AAT) and data exchange transceiver (DET). [b] A setup for one relay node.

the motion control algorithm and data acquisition unit of the robot.

Our objective is to facilitate smart navigation and wireless data transmission for the robot during operation. First, we explain the system hardware and then the operation procedure.

A. SYSTEM HARDWARE

Our proposed wireless robotic network includes:

- One wireless sensor module is mounted on the robot and moves with it during operation.
- Some fixed relay nodes (RN) above ground.

The wireless sensor module on the robot synchronizes the wireless sensor, micro-pump system, and the motion control units and we explained it earlier in this paper. We call the transceiver on the robot, moving transceiver (MT) for brevity. The RNs include two radio transceivers that are connected to the host MCU. One transceiver always advertises an address signal on the air and the other one exchanges data with the robot. We call the transceiver that advertises the signal, address advertiser transceiver (AAT), and the transceiver that exchanges data, data exchange transceiver (DET) (see Fig. 13). The RNs are located at special configurations of the pipeline like bend, wyes, and T-junction. Fig. 14 shows the overall view of the proposed wireless robotic sensor that the robot moves inside the pipeline underground and the RNs are located at special configurations of the pipeline above ground. Based on [10], it is possible to facilitate underground communication in few meters using electromagnetic waves. Also, the authors in [31], investigate the reliability of the communication link between the RN and the underground robot. The distance between the robot and the RNs is varied in different locations in the order of 1 m to 2 m according to the standards in the distribution systems [32]. Also, water is the most challenging environment in terms of signal propagation that attenuates radio signal

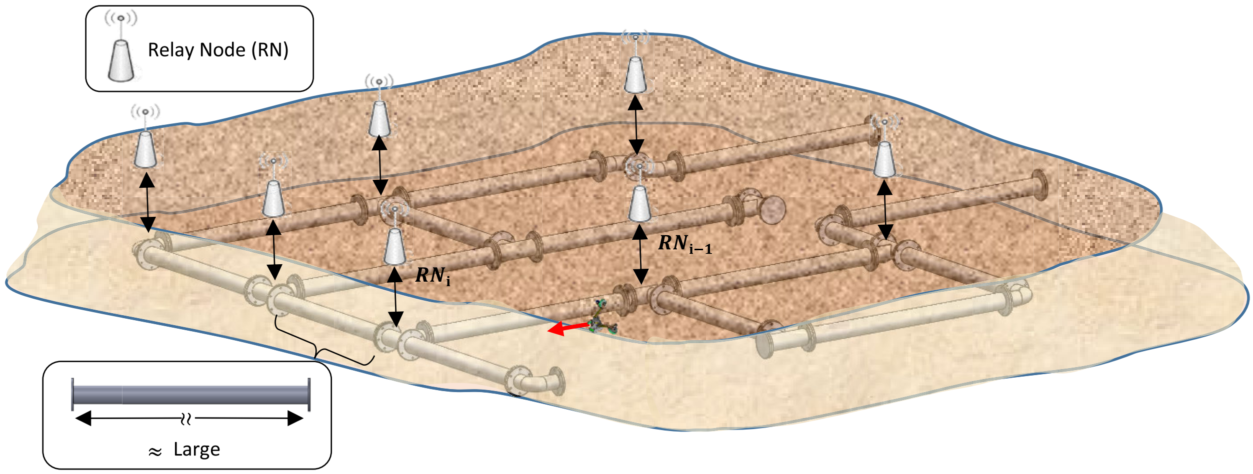

FIGURE 14. Overall view of our proposed robotic network. The robot moves inside pipe underground and the RNs are located at special configurations of the pipelines like bends and T-junctions. The distance between the RNs is large.

power. In our experiments in section IV, we achieved the read range of around 1 meter, if only water is the propagation environment. However, since the propagation environment is water, soil, and air, the read range of our wireless system is more than 1 m that fulfills the requirement of communication between the robot and RN. Since, the properties of soil that affect signal attenuation [10] (i.e. water content, temperature, soil bulk density, sand/clay composition) are highly variable in different locations and the experiments in one location in soil could not represent all situations, we did our experiments in water that is most challenging. Hence, we can guarantee that the RN and the robot can establish wireless communication once they are close to the range of each other.

B. OPERATION PROCEDURE

The operation procedure of the robotic divides into five parts: 1) Motion in Straight Path with No Wireless Communication: The robot moves in a straight path between two consecutive RNs (RN_{i-1} to RN_i) and it does not have wireless communication (see Fig. 15).

2) Establishing Communication between the Robot and RN_i: The robot establishes wireless communication with RN_i when the robot arrives in the radio range of RN_i.

3) Sensor Measurement, Processing, and Wireless Transmission from the Robot to the RN_i:

The robot starts sensor measurements, processes and transmits them to the RN_i.

4) Wireless Transmission from the RN_i to the Robot:

The RN_i transmits the motion control command to the robot.

5) Change of Direction of the Robot:

After the robot received the motion command signal, it changes its direction and starts moving in a straight path until it arrives at the radio range of the RN_{i+1}.

The operation procedure of the robot is in a way that the robot switches between different control algorithm modes and data transmission directions. In the following, we explain each part of the procedure in detail.

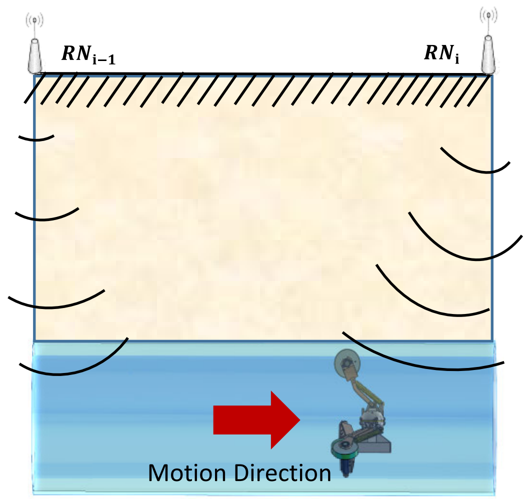

FIGURE 15. Part 1 of the proposed operation procedure: The robot moves from RN_{i-1} to RN_i and the robot does not have wireless communication with relay nodes.

1) MOTION IN A STRAIGHT PATH WITH NO WIRELESS COMMUNICATION

In this phase of the operation, the robot moves in a straight path and does not have wireless communication with RNs. The motion controller in this phase stabilizes the robot and makes it track a constant velocity. To have a measure of stabilization for the robot, we define rotation around the y-axis (ϕ), z-axis (ψ), and their derivatives, $\dot{\phi}$ and $\dot{\psi}$ (see Fig. 16). The controller effort for the stabilization task is to keep the stabilizing states of the robot, $\left[\phi\ \psi\ \dot{\phi}\ \dot{\psi}\right]$ at zero [9], [21]. To this aim, we designed a controller that is the linear quadratic regulator (LQR) and stabilizes the robot. Also, the robot needs to track the desired velocity during operation. To this aim, another controller is proposed which is

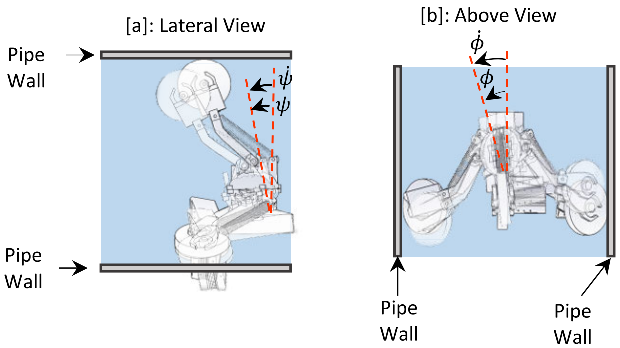

FIGURE 16. **Stabilizing states of the robot.**

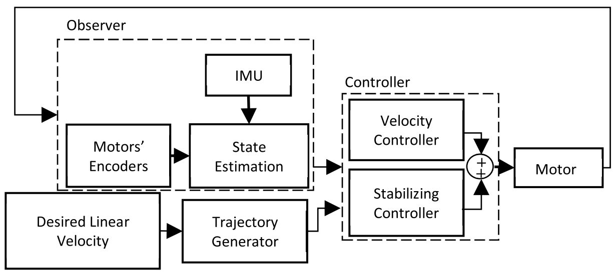

FIGURE 17. **The controller to stabilize the robot and track the desired velocity in straight paths.**

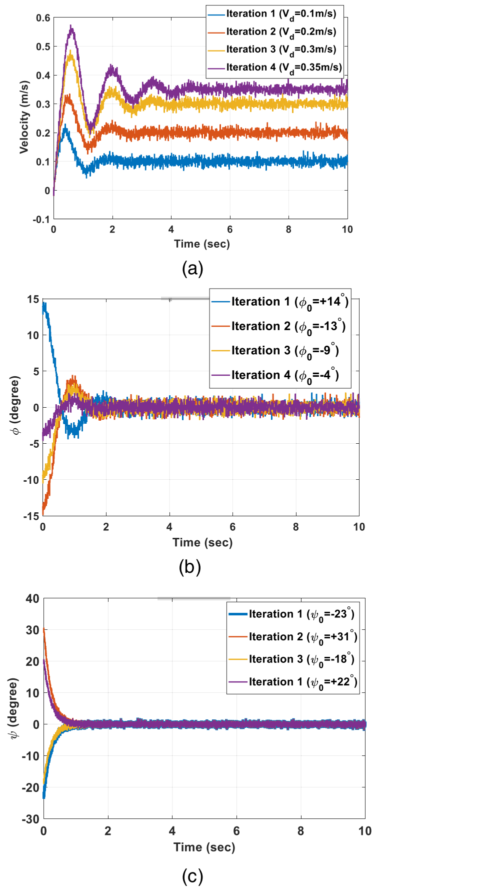

FIGURE 18. **The proposed LQR-PID based controller performance in straight path based on experimental results. Four iterations are done to validate the performance of the controller. (a) Linear velocity of the robot along pipe axis. (b) ϕ (degree). (c) ψ (degrees).**

based on a proportional-derivative-integral (PID) controller. If all the three wheels of the robot have equal angular velocity, the linear velocity of the robot is calculated based on one wheel's angular velocity. So, to have a defined linear velocity, we proposed three PID controllers to control the velocity of each wheel. The LQR and PID controllers are combined to fulfill both requirements in a straight path. Fig. 17 shows the controller algorithm diagram in this phase [9], [25]. The the observer in the controller algorithm fuses the data from an inertial measurement unit (IMU) which is placed in the central processor and three encoders at the end of the wheels. The encoders measure the angular velocity of the wheels. Hence with this architecture, we have a sense of orientation of the robot and odometry for it. We validated the performance of the controller in this phase with experimental results. To this aim, we performed four iterations with different desired linear velocities, V_d, and initial values for ϕ, ϕ_0 and ψ, ψ_0. In Table 3, the specifications of each iteration are defined. The performance of the controller in this phase is shown in Fig. 18. For the linear velocity, the robot starts from zero velocity and reaches the desired velocity. Also for the stabilizing states, the initial deviations are canceled and kept at that point with small fluctuation (see Fig. 18).

The results show the LQR-PID controller can stabilize the robot in the pipeline and makes the robot track the desired velocity [9].

2) ESTABLISHING COMMUNICATION BETWEEN THE ROBOT AND RN_i

In the pipeline underground, the robot is moving in a straight path inside the pipe from RN_{i-1} toward RN_i. On the ground in RN_i, one transceiver on the RN_i is in transmit mode and advertises the RN_i's location order continuously. The location order is the address of the RN_i in the network that we call "relay node address" or RNA in short. For example, the RN_1 is the first relay node in the network in which the robot approaches to and the RNA for it (i.e. RN_1) is 1. The RN_2 is the second one in the network and its RNA (i.e. RN_2) is 2, and so on. Since each RN advertises a unique RNA, the possible overlap between radio signals of multiple RNs does not confuse the robot.

On the robot side, the robot needs to distinguish the right RN in the network. This way it can switch to the right control algorithm that facilitates efficient motion during operation. In other words, the robot needs a map of the operation path. Our solution to give the robot a sense of the map of the pipeline is to put the RNs in the special configurations of the pipeline network and give the robot an array that contains the RNAs and their orders in the network:

$$\mathbf{RNA} = \begin{bmatrix} RNA_1 & RNA_2 & \dots & RNA_n \end{bmatrix} \tag{14}$$

In (14), the RN_i reveals the information about the configuration type. The configuration type can be 90° bend,

Algorithm 1: Pipe Configuration Type Determination Steps in Phase 2 of the Operation Procedure

```
If (wireless_flag) {
        wireless_flag = 0;
        CT = 0; CT:: Configuration Type
        done = 0;
        i = 1;
while (!done){
    If (RNA_i == RNA){
        CT= RNA_i
        done = 1;}
    else
        {i = i + 1};
    end
 }
Interrupt_Service_Routine{
wireless_flag = 1;
}
```

45° bend, 135° bend, T-junction, etc. The robot is programmed in a way that knows the configuration shape associated with specific RNA. For example, the configuration associated with *RN*2 is a 90°-bend. Hence, the control algorithm chooses the control phase that steers the robot in a bend shape pipe. Fig. 19 shows the advertised RNA and the array in the robot's firmware. Algorithm 1 defines the configuration type of the pipe where the robot is located. The Interrupt_Service_Routine (i.e. built-in function in MCUs) in the algorithm is triggered once *RNA* is received by the wireless sensor module on the robot. The Interrupt_Service_Routine sets a defined flag so-called *wireless_flag* that triggers the process of defining the configuration type. First, the *wireless_flag* is unset for the next interrupt of the wireless sensor module, then a variable, *CT*, is defined to store the value of configuration type and finally, two variables, *done* and *i* are defined that stops the searching process and counts for the elements in **RNA** matrix, respectively. In the searching process, *RNA* is compared to the elements of **RNA** matrix; if the i^{th} element, RNA_i, matched *RNA*, RNA_i is stored in *CT* and the searching process stops by setting *done*. The motion controller [9]. The motion controller in this part of the procedure is stabilizer controller in which the performance of the controller is similar to Fig. 18 with the difference that the linear velocity is zero in this phase. Hence, we localize the robot in the network with the wireless communication and the map of the operation in the robot's firmware.

3) SENSOR MEASUREMENT, PROCESSING, AND WIRELESS TRANSMISSION FROM THE ROBOT TO THE RN_i

So far, the robot has received an *RNA*, stopped moving, and defined the configuration type. At this point, the micro-pump system activates and provides water samples for the onboard water quality monitoring sensors. To activate the micro-pump, a pin on the micro-pump driver (see Fig. 2) is

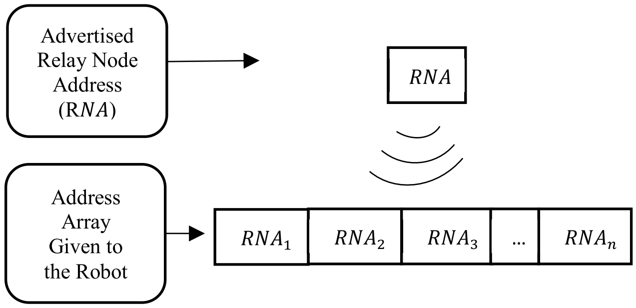

FIGURE 19. Advertised RNA and the address array that is programmed in the robot firmware.

Algorithm 2: Phase 3 of the Operation for Sensors Measurement, Processing, and Transmission

1. Micro-pump Activation.
2. Idle State for One Minute (Sensors' Output Settlement)
3. ADC Activation (Start Sensor Measurement).
4. Sensor Measurement Processing.
5. Data Packet Creation (Compatible with Communication Protocol).
6. Update the MT's Payload with Data Packet.
7. RX Mode → TX Mode.
8. Data Packets Transmission.))
9. Done Transmission (DT) Variable.))
10. TX Mode → RX Mode.

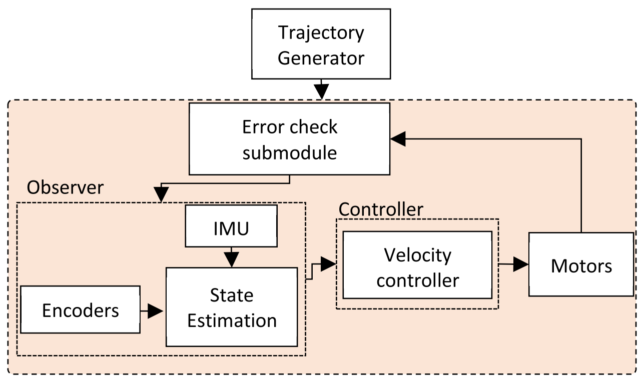

FIGURE 20. The motion control algorithm for non-straight paths.

set and the driver activates the micro-pump with the constant flowrate of 7 ml/min. The quality monitoring sensors are chemical sensors (the number of the sensors depends on the application.) that are designed and developed by our team [5]. These chemical sensors operate based on chemical reactions and their output converges to a specific value after around one minute [5]. The firmware remains idle for one minute and no function is implemented during this time and also the robot remains in the stabilized configuration with zero velocity until the output of the sensors settle. The sensors are connected to the host MCU. After their output is settled, the analog to digital conversion (ADC) unit of the MCU starts sensor measurements. The MCU then processes raw sensor data to compute the real value of the target analyte. The processing

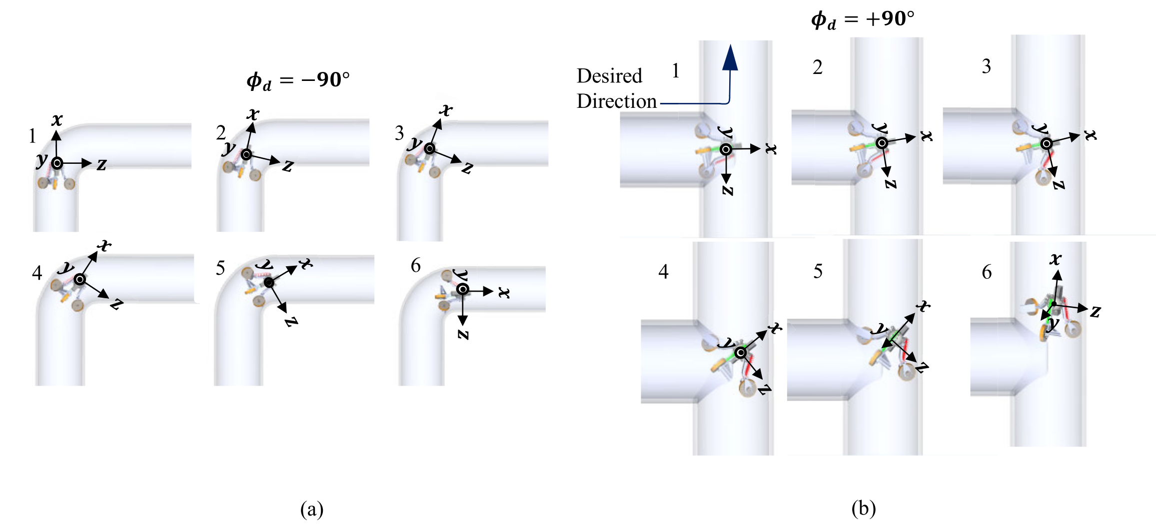

FIGURE 21. DAMS-MATALB co-simulation results for (a) 90° Bend and (b) T-junction based on Non-straight controller.

TABLE 3. Experiment specifications in four iterations for phase 1 of the motion controller.

Iteration	V_d (m/s)	ϕ_0(degree)	ψ_0(degree)
1	0.1	+14	-15
2	0.2	-13	-11
3	0.3	-9	+5
4	0.35	-3	+3

includes filtering noisy data, converting current to voltage, and applying the associated chemical formula to calculate the real value for the target analyte. Then a data packet that is compatible with the communication protocol is created that is an array that includes the preamble bytes, packet length, the packet counter, and processed sensor data. The payload of the MT is then updated with the data packet. The MCU at this state goes to transmit mode and transmits the data packets to the RN_i. The transceiver on the RN_i which is in receive mode, receives the packet. After the MCU transmits all data packets, it sends a separate data packet that includes a variable called Done Transmission (DT) to the RN_i, to acknowledge that the data packets are sent completely, and then MT goes to receive mode. Algorithm 2 shows the procedure in phase 3 that is related to the sensor measurement, processing, and transmission.

4) WIRELESS TRANSMISSION FROM RN_i TO THE ROBOT

In this phase, the RN_i sends a motion control command to the MT. Based on the configuration type that is already defined in part 2 of the operation, the robot chooses the control phase designed for non-straight configuration that steers the robot in the desired direction. Based on the literature, non-straight configurations are a challenge for in-pipe robots to pass through and require appropriate motion controllers [8], [33]–[41]. We propose a new controller that facilitates rotation for the in-pipe robot based on the differential motion for the wheels. The controller includes a

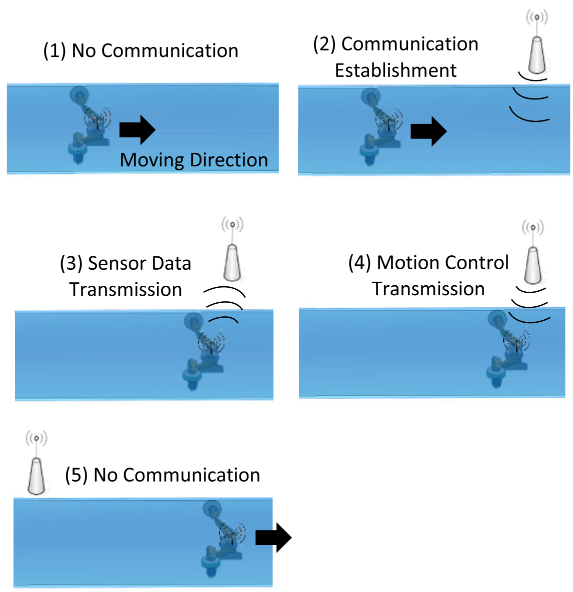

FIGURE 22. Wireless communication switching in the proposed operation procedure for the wireless robotic network.

trajectory generator block, an observer block, an error-check sub-module, and a velocity controller based on three PID controller. The trajectory generator creates differential motion in which different angular velocities for the wheels, change the direction of motion of the robot. The error-check sub-module monitors the amount of rotation around the desired axis and allows the controller in the non-straight phase to continue until the defined amount of rotation is acquired. Fig. 20 shows the control algorithm for the non-straight configuration. To evaluate the performance of this phase of the controller, we modeled the robot in AMDAS software which is a multibody dynamic simulator, and implemented the controller in the MATLAB Simulink environment. Then we linked the control plant in MATLAB and the simulated system in ADAMS software and co-simulated the robot-controller. Fig. 21 shows the motion sequences of the robot

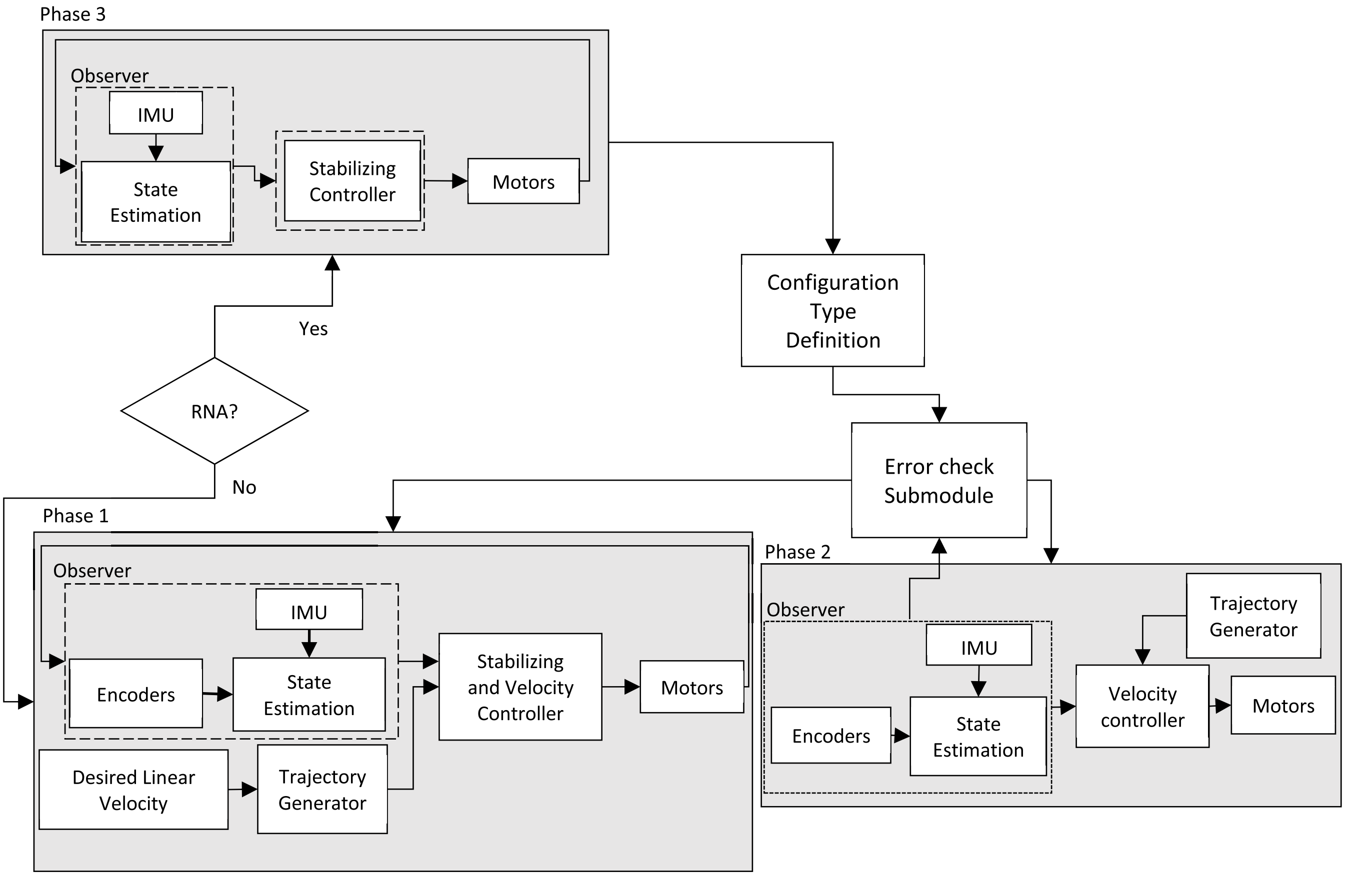

FIGURE 23. Synchronized wireless communication system with the multi-phase motion control algorithm. Switching between different phases of the motion control algorithm is performed with wireless system.

in bend and T-junction. The results in Fig. 21 prove that the motion control phases for the robot in T-junctions and bends can facilitate smooth motion for the robot in bends and T junctions. We repeated our simulations and validated the robot can cover bends with diameters range 9-in to 22-in and also T-junctions with diameters ranging from 9-in to around 15-in. Once the rotation is completed, the robot is located in a straight path and continues moving in a straight path. The control phase here is again the stabilizer-velocity tracking controller in Fig. 17.

5) CHANGE OF DIRECTION OF THE ROBOT

The robot switches to the non-straight controller phase and changes its direction to the desired direction. The robot communication with RN_i stops during rotation and RN_i is removed from the service. Fig. 22 shows switching between different motion control phases and communication direction modes during operation.

We synchronized the wireless communication setup and the motion control algorithm in this work. Fig. 23 shows the overall view of the synchronized wireless control for the operation procedure of the robot. Hence, the robot navigates between different configurations of the pipelines with the synchronization of the wireless sensor module and the multi-phase motion control algorithm.

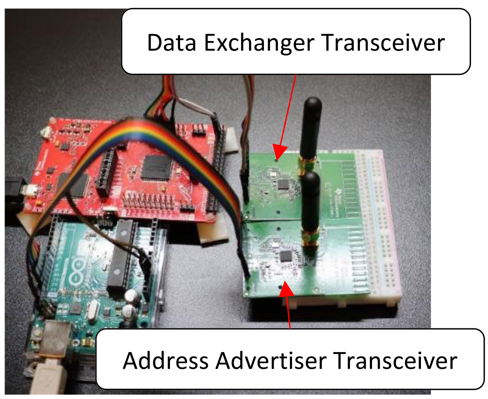

FIGURE 24. A setup for one relay node. Each relay node (RN) comprises two parts: Address advertiser transceiver (AAT) and data exchange transceiver (DET). Two CC1200 evaluation modules are connected to two MCU Launchpads.

C. EXPERIMENT

In this part, we evaluate the performance of the developed operation procedure with the experiment. To this aim, a relay node is proposed with two CC1200 evaluation modules in 434 MHz that are connected to the two MCU Launchpads (see Fig. 25). The robot is located in a 14-in diameter pipe. Our goal is to investigate the functionality of the wireless control and navigation method. In other words, we validate

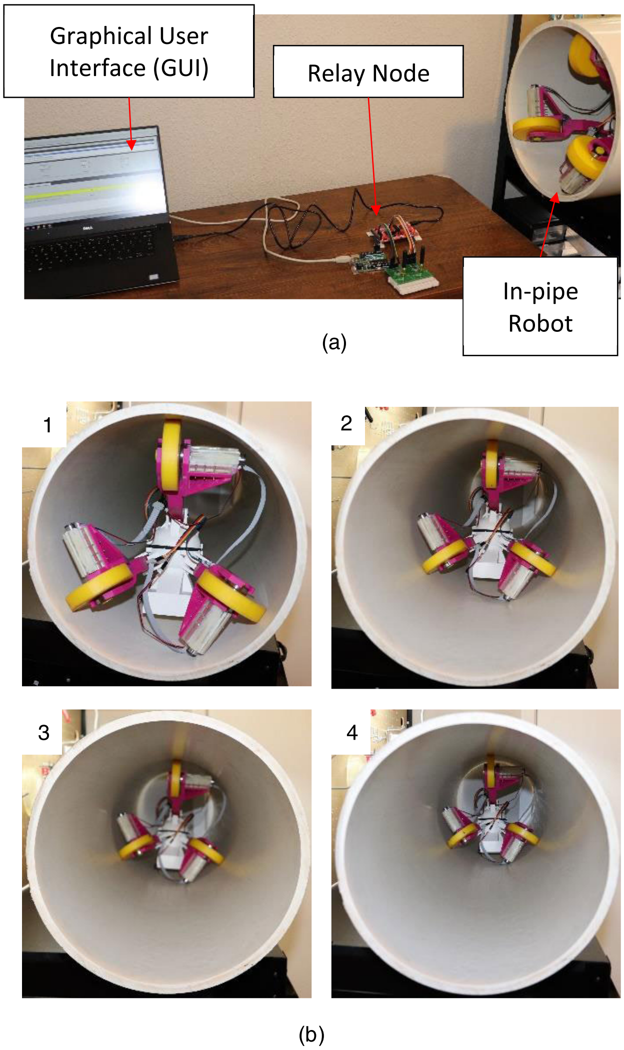

FIGURE 25. **(a) Experiment Setup: The in-pipe robot is located in a 14-in diameter PVC pipe. The relay node is connected to PC and the sends the *RNA* = 1 once the robot received at the end of the pipe. (b) Sequence of motion of the robot. The robot starts moving in (1) with phase 1 of the motion controller (stabilizer-velocity tracking controller) and reach to 10 cm/s velocity. Once the robot arrived at the end of the pipe, the relay node sends *RNA* = 1 and the robot stops with stabilized configuration.**

if switching between phases of motion control occurs by the proposed wireless control method. To this aim, the relay node sends the "start command" to the robot and the robot starts motion with phase 1 of the controller (stabilizer-velocity tracking controller) and moves inside the pipe with 10 cm/s. The robot has the map of the operation as $\mathbf{RNA} = [1]$ as we have just one junction in our experiment. The relay node sends the $RNA = 1$ when the robot reaches the end of the pipe and it is expected that the robot stops at this location once it received the *RNA*. We performed the experiment and the results are shown in Fig. 26 in which the sequences of motion are shown from 1 to 4. The robot first stabilizes itself at the beginning of the motion and reaches the desired velocity (i.e. 10 cm/s) and moves with stabilized motion in the pipe. At the end of the motion, the relay node sent the $RNA = 1$ and upon transmission, the robot stopped there with the stabilized configuration. Hence, the robot switched from phase 1 to phase 2 of the motion controller and the developed wireless control is verified.

1) LIMITATION OF THE STUDY

In our experiments, we found out that the time at which the AAT sends the *RNA* is extremely important as the robot stops with the stabilized configuration once it receives the *RNA*. In other words, switches to another phase of the motion control algorithm. In some experiments, the robot stopped near the end of the pipe (desired location) while in other experiments, the robot stopped at other undesired locations. This is because the radio signal propagates spatially in the air and the robot may receive it at any location. This phenomenon is higher in our experiment than in water medium in which water medium limits the read range of the radio signal is not present and in real applications, this effect is less than in our experiment but still exists. We can address the issue by locating a rangefinder sensor in front of the robot and find the distance from the front obstacle and reach close enough to the junction with the stabilized motion (phase 1) in a straight path before switching to phase 2 of the motion controller.

V. DISCUSSION AND CONCLUSION

The developed operation procedure facilitates localization and navigation in complicated configurations of pipelines for the in-pipe robots that was a challenge in this field. Also, the proposed method facilitates long-distance inspection for the robot; since the distance between the relay nodes is large. The resilient of the robot that is coined and discussed in [22] is considered in this robot in which the spring mechanism that provides friction force between the pipe wall and the wheels is characterized based on the extreme operating condition in in-service networks as well as the battery capacity of the robot. The spring mechanism prevents the robot from collapse during operation and the characterized battery ensures enough operation duration that is at least 3 hours in the conditions the robot moves with 50 cm/s against the water flow with 70 cm/s [9]. Even in case, the robot fails during operation, it is easy to pinpoint the location of the failed robot with this method. We also validated the operation procedure in each step separately by experiment and simulations; the performance of the motion controllers are validated with experiments in straight path and simulation in non-straight configurations, the reliability of the wireless communication system is validated to ensure it can penetrate harsh environments of water and pipe, bi- directionality, and fast discovery between the robot and the relay nodes. The sensors that measure the parameters of water have a rather long response time (around one minute [5]) and we considered their response time in the procedure. The developed procedure enables data transmission during operation which is useful in quality monitoring in long inspections. We also experimented with the wireless control to see its functionality to enable the robot for reliable motion in complicated configurations.

In our future work, we plan to do more field tests with the developed WSN in different networks and pipe configurations to evaluate the functionality of the system in the real application.

REFERENCES

[1] A. L. Vickers, "The future of water conservation: Challenges ahead," *J. Contemp. Water Res. Educ.*, vol. 114, no. 1, p. 8, 1999.

[2] E. Canada, *Threats to Water Availability in Canada*. Burlington, ON, USA: National Water Research Institute Burlington, 2004.

[3] D. Chatzigeorgiou, K. Youcef-Toumi, and R. Ben-Mansour, "Design of a novel in-pipe reliable leak detector," *IEEE/ASME Trans. Mechatronics*, vol. 20, no. 2, pp. 824–833, Apr. 2015, doi: 10.1109/TMECH.2014.2308145.

[4] R. Fletcher and M. Chandrasekaran, "SmartBall: A new approach in pipeline leak detection," in *Proc. 7th Int. Pipeline Conf.*, vol. 2, Jan. 2008, pp. 117–133, doi: 10.1115/IPC2008-64065.

[5] R. Wu, W. W. A. Wan Salim, S. Malhotra, A. Brovont, S. Pekarek, M. K. Banks, and D. M. Porterfield, "Self-powered mobile sensor for in-pipe potable water quality monitoring," in *Proc. 17th Int. Conf. Miniaturized Syst. Chem. Life Sci.*, 2013, pp. 14–16.

[6] D. M. Chatzigeorgiou, K. Youcef-Toumi, A. E. Khalifa, and R. Ben-Mansour, "Analysis and design of an in-pipe system for water leak detection," in *Proc. 37th Design Autom. Conf., A B*, vol. 5, Jan. 2011, pp. 1007–1016, doi: 10.1115/detc2011-48395.

[7] K. Miyasaka, G. Kawano, and H. Tsukagoshi, "Long-mover: Flexible tube in-pipe inspection robot for long distance and complex piping," in *Proc. IEEE/ASME Int. Conf. Adv. Intell. Mechatronics (AIM)*, Jul. 2018, pp. 1075–1080, doi: 10.1109/AIM.2018.8452690.

[8] Y. Qu, P. Durdevic, and Z. Yang, "Smart-Spider: Autonomous self-driven in-line robot for versatile pipeline inspection," *IFAC-PapersOnLine*, vol. 51, no. 8, pp. 251–256, 2018, doi: 10.1016/j.ifacol.2018.06.385.

[9] S. Kazeminasab, A. Akbari, R. Jafari, and M. K. Banks, "Design, characterization, and control of a size adaptable in-pipe robot for water distribution systems," in *Proc. 22nd IEEE Int. Conf. Ind. Technol. (ICIT)*, Mar. 2021, pp. 39–46, doi: 10.1109/ICIT46573.2021.9453583.

[10] I. F. Akyildiz and E. P. Stuntebeck, "Wireless underground sensor networks: Research challenges," *Ad Hoc Netw.*, vol. 4, no. 6, pp. 669–686, Nov. 2006, doi: 10.1016/j.adhoc.2006.04.003.

[11] S. Kazeminasab, M. Aghashahi, R. Wu, and M. K. Banks, "Localization techniques for in-pipe robots in water distribution systems," in *Proc. 8th Int. Conf. Control, Mechatronics Autom. (ICCMA)*, Nov. 2020, pp. 6–11, doi: 10.1109/ICCMA51325.2020.9301560.

[12] D. Wu, D. Chatzigeorgiou, K. Youcef-Toumi, S. Mekid, and R. Ben-Mansour, "Channel-aware relay node placement in wireless sensor networks for pipeline inspection," *IEEE Trans. Wireless Commun.*, vol. 13, no. 7, pp. 3510–3523, Jul. 2014, doi: 10.1109/TWC.2014.2314120.

[13] B. H. Lee and R. A. Deininger, "Optimal locations of monitoring stations in water distribution system," *J. Environ. Eng.*, vol. 118, no. 1, pp. 4–16, Jan. 1992, doi: 10.1061/(ASCE)0733-9372(1992)118:1(4).

[14] D. Wu, D. Chatzigeorgiou, K. Youcef-Toumi, and R. Ben-Mansour, "Node localization in robotic sensor networks for pipeline inspection," *IEEE Trans. Ind. Informat.*, vol. 12, no. 2, pp. 809–819, Apr. 2016, doi: 10.1109/TII.2015.2469636.

[15] J. A. I. Diaz, M. I. Ligeralde, M. A. B. Antonio, P. A. R. Mascardo, J. M. Z. Maningo, A. H. Fernando, R. R. P. Vicerra, E. P. Dadios, and A. A. Bandala, "Development of an adaptive in-pipe inspection robot with rust detection and localization," in *Proc. TENCON IEEE Region Conf.*, Oct. 2018, pp. 2504–2509, doi: 10.1109/TENCON.2018.8650073.

[16] A. V. Reyes-Acosta, I. Lopez-Juarez, R. Osorio-Comparan, and G. Lefranc, "3D pipe reconstruction employing video information from mobile robots," *Appl. Soft Comput.*, vol. 75, pp. 562–574, Feb. 2019, doi: 10.1016/j.asoc.2018.11.016.

[17] A. Dehghan Tezerjani, M. Mehrandezh, and R. Paranjape, "4-DOF pose estimation of a pipe crawling robot using a collimated laser, a conic mirror, and a fish-eye camera," in *Proc. Southwest Symp. Image Anal. Interpretation*, Apr. 2014, pp. 45–48, doi: 10.1109/SSIAI.2014.6806025.

[18] K. Ma, M. Schirru, A. H. Zahraee, R. Dwyer-Joyce, J. Boxall, T. J. Dodd, R. Collins, and S. R. Anderson, "PipeSLAM: Simultaneous localisation and mapping in feature sparse water pipes using the Rao-Blackwellised particle filter," in *Proc. IEEE Int. Conf. Adv. Intell. Mechatronics (AIM)*, Jul. 2017, pp. 1459–1464, doi: 10.1109/AIM.2017.8014224.

[19] J.-S. Lee, S.-G. Roh, D. W. Kim, H. Moon, and H. R. Choi, "In-pipe robot navigation based on the landmark recognition system using shadow images," in *Proc. IEEE Int. Conf. Robot. Autom.*, May 2009, pp. 1857–1862, doi: 10.1109/ROBOT.2009.5152724.

[20] S. Kazeminasab, M. Aghashahi, and M. K. Banks, "Development of an inline robot for water quality monitoring," in *Proc. 5th Int. Conf. Robot. Autom. Eng. (ICRAE)*, Nov. 2020, pp. 106–113, doi: 10.1109/ICRAE50850.2020.9310805.

[21] S. Kazeminasab, R. Jafari, and M. K. Banks, "An LQR-assisted control algorithm for an under-actuated in-pipe robot in water distribution systems," in *Proc. 36th Annu. ACM Symp. Appl. Comput.*, Mar. 2021, pp. 811–814, doi: 10.1145/3412841.3442097.

[22] W. J. Zhang and C. A. van Luttervelt, "Toward a resilient manufacturing system," *CIRP Ann.*, vol. 60, no. 1, pp. 469–472, 2011, doi: 10.1016/j.cirp.2011.03.041.

[23] K. Sattlegger and U. Denk, "Navigating your way through the RFID jungle," Texas Instrum., Dallas, TX, USA, White Paper, 2014.

[24] (2013). *CC1200 CC1200 Low-Power, High-Performance RF Transceiver 1 Device Overview*. Accessed: Sep. 29, 2020. [Online]. Available: www.ti.com

[25] Z. Chu, F. Zhou, Z. Zhu, R. Q. Hu, and P. Xiao, "Wireless powered sensor networks for Internet of Things: Maximum throughput and optimal power allocation," *IEEE Internet Things J.*, vol. 5, no. 1, pp. 310–321, Feb. 2018, doi: 10.1109/JIOT.2017.2782367.

[26] S. Kazeminasab, R. Jafari, and M. K. Banks, "SmartCrawler: An in-pipe robotic system with wireless communication in water distribution systems," 2021, *arXiv:2105.06344*. [Online]. Available: http://arxiv.org/abs/2105.06344

[27] A. U. Alam, D. Clyne, H. Jin, N.-X. Hu, and M. J. Deen, "Fully integrated, simple, and low-cost electrochemical sensor array for *in situ* water quality monitoring," *ACS Sensors*, vol. 5, no. 2, pp. 412–422, Feb. 2020, doi: 10.1021/acssensors.9b02095.

[28] H. Guo, Z. Sun, and C. Zhou, "Practical design and implementation of metamaterial-enhanced magnetic induction communication," *IEEE Access*, vol. 5, pp. 17213–17229, 2017, doi: 10.1109/ACCESS.2017.2719406.

[29] Z. Sun, P. Wang, M. C. Vuran, M. A. Al-Rodhaan, A. M. Al-Dhelaan, and I. F. Akyildiz, "MISE-PIPE: Magnetic induction-based wireless sensor networks for underground pipeline monitoring," *Ad Hoc Netw. J.*, vol. 9, no. 3, pp. 218–227, 2011, doi: 10.1016/j.adhoc.2010.10.006.

[30] S. Kisseleff, I. F. Akyildiz, and W. H. Gerstacker, "Throughput of the magnetic induction based wireless underground sensor networks: Key optimization techniques," *IEEE Trans. Commun.*, vol. 62, no. 12, pp. 4426–4439, Dec. 2014, doi: 10.1109/TCOMM.2014.2367030.

[31] D. Wu, K. Youcef-Toumi, S. Mekid, and R. Ben Mansour, "Relay node placement in wireless sensor networks for pipeline inspection," in *Proc. Amer. Control Conf.*, Jun. 2013, pp. 5905–5910, doi: 10.1109/ACC.2013.6580764.

[32] R. Book, "Guidelines for human settlement planning and design," *Compil. Under Patronage SA Dep. Hous. CSIR Build. Constr. Technol. Div.*, to be published.

[33] H.-P. Huang, J.-L. Yan, and T.-H. Cheng, "Development and fuzzy control of a pipe inspection robot," *IEEE Trans. Ind. Electron.*, vol. 57, no. 3, pp. 1088–1095, Mar. 2010, doi: 10.1109/TIE.2009.2031671.

[34] A. H. Heidari, M. Mehrandezh, R. Paranjape, and H. Najjaran, "Dynamic analysis and human analogous control of a pipe crawling robot," in *Proc. IEEE/RSJ Int. Conf. Intell. Robots Syst.*, Oct. 2009, pp. 733–740, doi: 10.1109/IROS.2009.5354801.

[35] W. Zhao, L. Zhang, and J. Kim, "Design and analysis of independently adjustable large in-pipe robot for long-distance pipeline," *Appl. Sci.*, vol. 10, no. 10, p. 3637, May 2020, doi: 10.3390/app10103637.

[36] H. Takeshima and T. Takayama, "Development of a steerable in-pipe locomotive device with six braided tubes," *ROBOMECH J.*, vol. 5, no. 1, pp. 1–11, Dec. 2018, doi: 10.1186/s40648-018-0127-5.

[37] A. A. Bandala, J. M. Z. Maningo, A. H. Fernando, R. R. P. Vicerra, M. A. B. Antonio, J. A. I. Diaz, M. Ligeralde, and P. A. R. Mascardo, "Control and mechanical design of a multi-diameter tri-legged in- pipe traversing robot," in *Proc. IEEE/SICE Int. Symp. Syst. Integr. (SII)*, Jan. 2019, pp. 740–745, doi: 10.1109/SII.2019.8700363.

[38] A. Kakogawa and S. Ma, "Design of a multilink-articulated wheeled pipeline inspection robot using only passive elastic joints," *Adv. Robot.*, vol. 32, no. 1, pp. 37–50, Jan. 2018, doi: 10.1080/01691864.2017.1393348.

[39] L. Brown, J. Carrasco, S. Watson, and B. Lennox, "Elbow detection in pipes for autonomous navigation of inspection robots," *J. Intell. Robotic Syst.*, vol. 95, no. 2, pp. 527–541, Aug. 2019, doi: 10.1007/s10846-018-0904-7.

[40] W. He, Z. Li, and C. L. P. Chen, "A survey of human-centered intelligent robots: Issues and challenges," *IEEE/CAA J. Autom. Sinica*, vol. 4, no. 4, pp. 602–609, Oct. 2017, doi: 10.1109/JAS.2017.7510604.

[41] X. Yu, W. He, H. Li, and J. Sun, "Adaptive fuzzy full-state and output-feedback control for uncertain robots with output constraint," *IEEE Trans. Syst., Man, Cybern. Syst.*, early access, Feb. 3, 2020, doi: 10.1109/TSMC.2019.2963072.

SABER KAZEMINASAB (Graduate Student Member, IEEE) received the B.Sc. degree in mechanical engineering from Iran University of Science and Technology, Tehran, Iran, in 2014, and the M.Sc. degree in mechatronics engineering from the University of Tehran, Tehran, in 2017. He is currently pursuing the Ph.D. degree with the Department of Electrical and Computer Engineering, Texas A&M University, College Station, TX, USA. His research interests include mechatronics, robotics, control theories, mechanism design, and actuator design.

M. KATHRINE BANKS received the B.Sc. degree in engineering from the University of Florida, the M.Sc. degree in engineering from the University of North Carolina, and the Ph.D. degree in civil and environmental engineering from Duke University, in 1989. She is currently a Professor with the Civil Engineering Department. She is also the President of the Texas A&M University, where she helped to establish the EnMed Program (led by Roderic Pettigrew, Ph.D., and M.D.), an Innovative Engineering Medical School Option created by Texas A&M University and Houston Methodist Hospital, designed to educate a new kind of physician who will create transformational technology for health care. Her research interests include applied microbial systems, biofilm processes, wastewater treatment and reuse, and phytoremediation bioremediation. She is an Elected Fellow of the American Society of Civil Engineers, was elected in 2014 to the National Academy of Engineering, and was formerly a Jack and Kay Hockema Professor at Purdue University. She is a recipient of the American Society of Civil Engineers Petersen Outstanding Woman of the Year Award, the American Society of Civil Engineers Rudolph Hering Medal, the Purdue Faculty Scholar Award, the Sloan Foundation Mentoring Fellowship, and the American Association of University Women Fellowship. In February 2019, she was named to the Board of Directors of Halliburton.